Hanlon, S. (1961), Ph.D. dissertation, University of California, Berkeley.
Hanlon, S., and Johnson, R. S. (1971), *Fed. Proc., Fed. Amer. Soc. Exp. Biol. 30*, 1096 Abstr.
Hearst, J. E., and Botchan, M. (1970), *Annu. Rev. Biochem. 39*, 151.
Huang, R. C. C., and Bonner, J. (1965), *Proc. Nat. Acad. Sci. U. S. 54*, 960.
Leloir, L. F., and Cardini, C. E. (1957), *Methods Enzymol. 3*, 843.
Li, H. J., and Bonner, J. (1971), *Biochemistry 10*, 1461.
Li, H. J., Isenberg, I., and Johnson, W. C., Jr. (1971), *Biochemistry 10*, 2587.
Lowry, O. H., Rosebrough, N. J., Farr, A. L., and Randall, R. J. (1951), *J. Biol. Chem. 193*, 265.
Marvin, D. A., Spencer, M., Wilkins, M. H. F., and Hamilton, L. D. (1961), *J. Mol. Biol. 3*, 547.
Maurer, H. R., and Chalkley, G. R. (1967), *J. Mol. Biol. 27*, 431.
Ohlenbusch, H. H., Olivera, B. M., Tuan, D., and Davidson, N. (1967), *J. Mol. Biol. 25*, 299.
Olins, D. E., and Olins, A. L. (1971), *J. Mol. Biol. 57*, 437.
Oster, G. (1948), *Chem. Rev. 43*, 319.
Pardon, J. F., Wilkins, M. H. F., and Richards, B. M. (1967), *Nature (London) 215*, 508.
Permogorov, V. I., Debabov, V. G., Sladkova, I. A., and Rebentish, B. A. (1970), *Biochim. Biophys. Acta 199*, 556.
Richards, B. M., and Pardon, J. F. (1970), *Exp. Cell. Res. 62*, 184.
Shih, T. Y., and Bonner, J. (1970), *J. Mol. Biol. 48*, 469.
Shih, T. Y., and Fasman, G. D. (1970), *J. Mol. Biol. 52*, 125.
Shih, T. Y., and Fasman, G. D. (1971), *Biochemistry 10*, 1675.
Shih, T. Y., and Fasman, G. D. (1972), *Biochemistry 11*, 398.
Simpson, R. T., and Sober, H. A. (1970), *Biochemistry 9*, 3103.
Smart, J. E., and Bonner, J. (1971a), *J. Mol. Biol. 58*, 651.
Smart J. E., and Bonner, J. (1971b), *J. Mol. Biol. 58*, 661.
Smart, J. E., and Bonner, J. (1971c), *J. Mol. Biol. 58*, 675.
Stellwagen, R. H., and Cole, R. D. (1969), *Annu. Rev. Biochem. 38*, 951.
Tuan, D. Y. H., and Bonner, J. (1969), *J. Mol. Biol. 45*, 59.
Tunis-Schneider, M. J., and Maestre, M. F. (1970), *J. Mol. Biol. 52*, 521.
Wagner, T., and Spelsberg, T. C. (1971), *Biochemistry 10*, 2599.
Zubay, G., and Doty, P. (1959), *J. Mol. Biol. 1*, 1.

Conformational Changes of Transfer Ribonucleic Acid. Equilibrium Phase Diagrams†

P. E. Cole, S. K. Yang, and D. M. Crothers*

ABSTRACT: We report systematic studies of the thermal denaturation of $tRNA_1^{Tyr}$, $tRNA^{fMet}$, $tRNA_2^{Phe}$, and $tRNA_1^{Val}$, all from *Escherichia coli*. Measurements at the absorbance maximum of 4-thiouridine show multiphasic melting curves at high salt (0.17 M Na^+, for example, no Mg^{2+}), and predominantly monophasic curves at low salt (0.005 M Na^+, for example, no Mg^{2+}). The variation of these transition midpoints with the logarithm of Na^+ concentration defines a phase diagram of four different conformational zones, with temperature and ion concentration as independent variables. There is no evidence for a separate Mg^{2+} zone of the phase diagram. When the low-salt conformation is converted to the high-salt form, the process has an activation energy between 25 and 61 kcal/mole, depending on the tRNA. We also report some characteristic spectral differences between the various conformational phases. In order to rationalize the conformational behavior, we propose a phase diagram in which the high-salt, low-temperature form is the "native" conformation, with tertiary structure. As the temperature is raised, the tertiary structure is lost, and the conformation at high salt and medium temperature is hypothesized to be "cloverleaf or close variant." At low temperature and low salt concentration, the tertiary structure is also lost; however, the product is not a "cloverleaf" but rather an "extended form" that has noncloverleaf secondary structure. When the temperature is raised sufficiently at both low and high salt concentration, the product is the randomly coiling single strand. From systematic examination of the influence of Mg^{2+} on thermal transitions, we conclude that it causes a marked stabilization of the tertiary structure present in high Na^+, but that it does not produce a new separately melting cooperative interaction unit.

Ribonucleic acids have complex conformational properties. For example, tRNA can exist in a metastable "denatured" conformation (Lindahl *et al.*, 1966; Gartland and Sueoka, 1966), from which biological activity can be recovered by heat treatment. Or, when native tRNA is gradually heated, a number of intermediate states are observed before the randomly coiling, single-strand conformation is reached at high temperatures (Riesner *et al.*, 1969). Another transition of particular interest is the loss of tertiary structure postulated by Fresco *et al.* (1966).

Study of these conformational changes is hampered by the lack of rigorous proof of any RNA conformation. Nucleic

† From the Department of Chemistry, Yale University, New Haven, Connecticut 06250. *Received June 9, 1972.* This is the first paper in a series. This research was supported by a grant (GM 12589) from the National Institutes of Health. D. M. C. holds a Career Development Award (GM 19978) from the same source. P. E. C. was supported by NIH Predoctoral Fellowship GM41629.

acids have yielded much more slowly than proteins to crystalographic analysis of three dimensional structure. Therefore it has been necessary to rely heavily on more indirect methods for studying structure, such as accessibility of particular nucleotides to chemical attack (Cramer, 1971), or binding of oligonucleotides complementary to particular sequences (Uhlenbeck *et al.*, 1970; Eisinger *et al.*, 1971).

The one generally agreed upon feature of tRNA conformation is the cloverleaf secondary structure (Cramer, 1971). The main reason for its wide acceptance is the striking fact that all known tRNA base sequences can be written in nearly the same cloverleaf pattern. Furthermore, none of the indirect structural studies provide evidence against the cloverleaf in native tRNA. Hence this secondary structure has been universally used as the basis for model building experiments on the three-dimensional or tertiary structure of tRNA (Arnott, 1971).

In our studies of tRNA conformational changes, we will also assume that the native structure is based on a cloverleaf. It is our view, however, that this assumption can be applied only to native tRNA, and not to partly melted intermediates. Thus when the native tertiary structure is melted by an increase of temperature or decrease of salt concentration, there is no reason to assume that the predominant secondary structure that remains has the cloverleaf bonding pattern. Close examination of any tRNA base sequence reveals many alternative bonding schemes, and these cannot be dismissed in any case except (by our assumption) fully native tRNA.

Our purpose in this paper is to report systematic studies of tRNA conformation as a function of temperature and ionic conditions. We do these by measuring thermal melting transitions at different salt concentrations. With appropriate measurements, well-defined melting steps can be observed, and these form the basis for a general phase diagram of conformation, with temperature and salt concentration as independent variables.

The regions of the phase diagram are clearly defined, but the more difficult question is the nature of the conformation in each phase. In this paper we present an interpretation of the phase diagram largely as a hypothesis, and leave for later papers in the series the accumulation of additional evidence that favors the hypothesis.

Finally, in considering tRNA conformational changes, the possible relation to biological function should be kept in mind. The physical mechanism of protein synthesis might, for example, require a flexible tRNA structure, which could be provided by conformational changes. Thus some, although probably not all, of the conformational changes exhibited by tRNA alone could be important for function, and it is appropriate to define what the possibilities are.

Materials and Methods

Buffers. Thermal transitions were measured at a number of salt concentrations, requiring a range of buffers. Most experiments used a buffer designated PCEP, containing 1 mM phosphate, sodium cacodylate (0.1–10 mM), Na_2EDTA (0.05–1 mM), and sufficient $NaClO_4$ (Fluka Chemical Co., puriss p.a. grade) to make the desired Na^+ concentration. (Perchlorate was chosen as the anion because the more usual chloride causes problems with the electrodes in temperature-jump experiments.) The molar Na^+ concentration is indicated by a number in front of PCEP; for example, 0.17 PCEP contains 0.17 M Na^+. All buffers were adjusted to pH 7.0 if necessary with small amounts of HCl or NaOH. Other specialized buffers are described in figure captions. Further details are given by Cole (1972) and Yang (1972).

tRNA Samples. $tRNA_1^{Tyr}$ (*Escherichia coli* K-12, CA 224) was purified from unfractionated tRNA by the methods described by Armstrong *et al.* (1969), Nishimura *et al.* (1967), and Yang (1972). The final preparations had tyrosine acceptor activities of 1550–1650 pmoles/A_{260} unit for $tRNA_1^{Tyr}$ (1700 pmoles/A_{260} unit is assumed to be 100% pure). $tRNA^{fMet}$, $tRNA_2^{Phe}$, and $tRNA^{Val}$ (*E. coli* K-12, MO7) were kindly donated by Oak Ridge National Laboratory. The specifications sent with the samples claimed the following activities: $tRNA^{fMet}$, 1413 pmoles/A_{260} unit; $tRNA_2^{Phe}$, 995 pmoles/A_{260} unit; and $tRNA_{Phe}^{Val}$, 1310 pmoles/A_{260} unit. We found $tRNA^{fMet}$, 1130 pmoles/A_{260} unit; $tRNA_2^{Phe}$, 950 pmoles/A_{260} unit; and $tRNA^{Val}$, 900 pmoles/A_{260} unit. Since the $tRNA^{Val}$ sample had the lowest purity, we checked the critical observations with a high purity sample (1630 pmoles/A_{260} unit) of $tRNA^{Val}$ (*E. coli* K-12, Ca 244) kindly provided by Dr. Lee Johnson.

tRNA stock solutions were stored at −80°. After dialysis against the appropriate buffer, solutions were kept frozen at −16° until use.

Acceptor activity assays were performed as described by Hoskinson and Khorana (1965), using ^{14}C-labeled amino acids obtained from New England Nuclear.

Precautions taken against nuclease contamination are described by Cole (1972).

Dialysis. Dialysis tubing was boiled in distilled water, then in three successive solutions of 5% sodium bicarbonate +1% EDTA, and once in 30% ethanol–water, then rinsed and boiled twice in water. Mg^{2+}-containing tRNA samples were dialyzed four times against a 100-fold excess of buffer containing 1 mM EDTA to remove the Mg^{2+}. Change of buffer was accomplished by thrice repeated dialysis against a 100-fold excess of the desired buffer.

Melting Curves. Thermal transition curves and other spectral measurements were made on a Cary Model 14 recording spectrophotometer equipped with a thermostatted cell compartment plus two slide-wires—an expanded scale, 0–0.1 and 0.1–0.2 absorbance, as well as a regular wire, 0–1 and 1–2 absorbance. The cell compartment was kept at 25.0° with a constant temperature bath. Neutral density filters, when used, were mounted in a holder contacting the cell compartment walls—this procedure allowed the filter to be kept at constant temperature and therefore avoided the slight absorbance change of the filter with temperature.

Samples were saturated with helium before being placed in water-jacketed, Teflon-stoppered, 1-cm pathlength spectrophotometer cells (Hellma QS 160). (The use of helium prevents bubble formation since its solubility does not decrease with increasing temperature; Felsenfeld and Sandeen, 1962.) The temperature differential between the cells and circulating bath was calibrated by placing a thermistor in the cell. In subsequent runs, the calibration curve allowed bath temperatures to be converted to cell temperatures.

Absorbance changes from the initial temperature were measured with the expanded scale slide-wire and a neutral density filter in the reference chamber, if needed. Thermal equilibrium was always attained before readings were taken. Absorbance drift after thermal equilibration (approximately 10 min) was not usually observed; its presence indicated cell leakage, spectrophotometer malfunction, or slow kinetic effects such as tRNA dimerization (Yang *et al.*, 1972).

Transition Midpoints. The melting temperature T_m was taken as the temperature at which the absorbance had

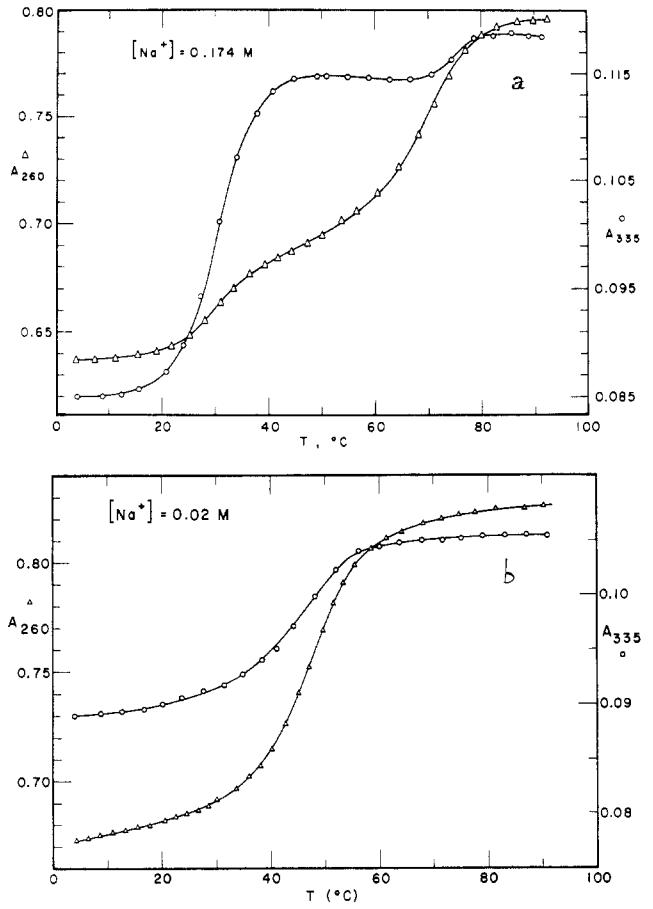

FIGURE 1: Comparison of melting curves for $tRNA_1^{Tyr}$ at high and low salt concentration. Absorbance measurements refer to tRNA samples at identical concentrations; the absorbance difference between low and high salt was determined by a salt-jump experiment; (a) melting in 0.17 PCEP, (△) measured at 260 nm; (○) measured at 335 nm; (b) melting in 0.02 PCEP, (△) measured at 260 nm; (○) measured at 335 nm.

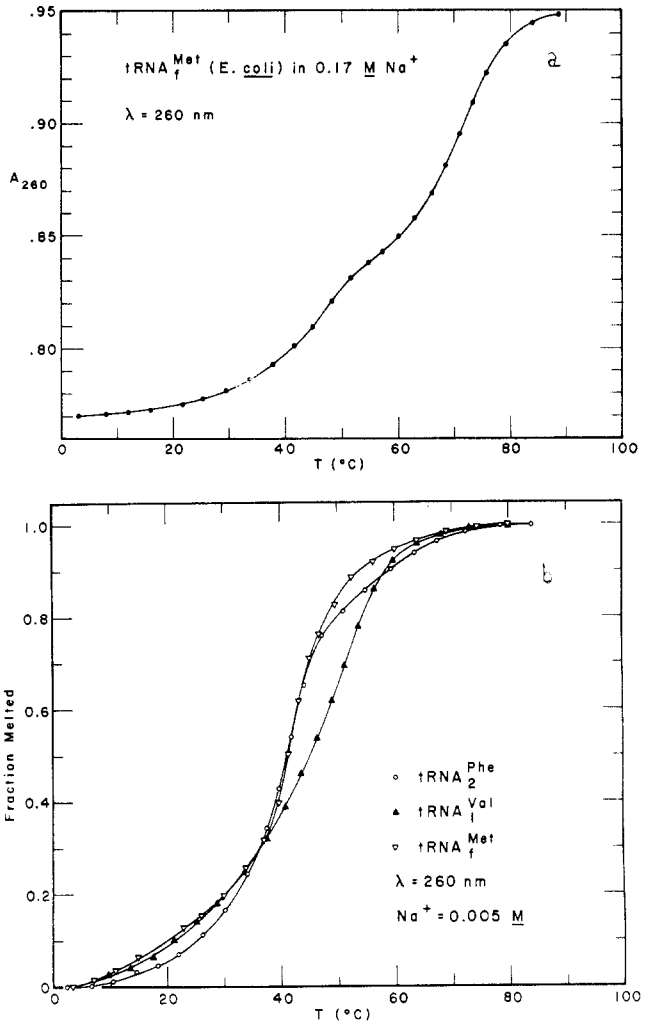

FIGURE 2: Comparison of high and low salt melting curves, measured at 260 nm: (a) $tRNA^{fMet}$ in 0.17 PCEP; (b) normalized melting curves for $tRNA_2^{Phe}$, $tRNA^{Val}$, and $tRNA^{fMet}$ in 0.005 PCEP. The "fraction melted" is the fraction of the total absorbance change (260 nm) from lowest to highest temperature that has occurred at temperature T.

risen half-way between its initial (A_i) and final (A_f) values. For monophasic transitions, A_i was measured at the lowest temperature, and A_f at the highest temperature in the standard melting curve procedure. When the transition was biphasic, A_f for the first transition (and A_i for the second transition) was taken at the intermediate temperature where dA/dT was a minimum.

Reversibility. Melting curves at 260 nm were generally found to be reversible within experimental error, but some evidence of irreversibility can be seen at 335 nm. In the case of $tRNA^{Tyr}$ this is extensive at high salt concentration (0.5 M) and is due to the dimerization reaction described previously (Yang *et al.*, 1972). Melting curves at 335 nm for $tRNA^{fMet}$ in 0.17 M Na^+ were nearly reversible. For example, after a sample (A_{335} = 0.26) had been heated to 88°, it was rapidly cooled, then heated slowly to 55°, and cooled again. Following this treatment, the optical density increase between 5 and 55° was 90% as large as in the first heating. At low salt concentration (0.005 M Na^+) the 335-nm melting curve of $tRNA^{fMet}$ was reversible within experimental error.

We also measured the amino acid acceptor activity of tRNA samples after melting. The maximum loss observed was 7%, except when Mg^{2+} was present, in which case exposure to high temperature (90°) caused more extensive degradation.

Salt-Jump Experiments. The addition of a concentrated salt solution to a tRNA solution constitutes a "salt-jump" experiment. The initial buffer was 0.02 PCEP or 0.005 PCEP, and the concentrated buffer added changed the composition to 0.17 PCEP. The salt solution was added with a micropipet, and the cell contents were mixed by inversion. When Mg^{2+} was added, EDTA was generally omitted from the buffer. For the fast kinetic experiment in which Mg^{2+} was added to tRNA in 0.17 M Na^+, mixing was accomplished with a micro stopped flow cell constructed after the design of Strittmatter (1964).

Solutions which had been "salt jumped" to 0.17 M Na^+ were melted and also assayed for acceptor activity, and found to be identical with samples that had been dialyzed into that buffer.

Results

tRNA Melting Curves Are Clearly Biphasic (or Multiphasic) at High Na^+ Concentration and Largely Monophasic at Low Na^+. Thermal transition curves for tRNA can be measured either by following the absorbance of the major bases (at

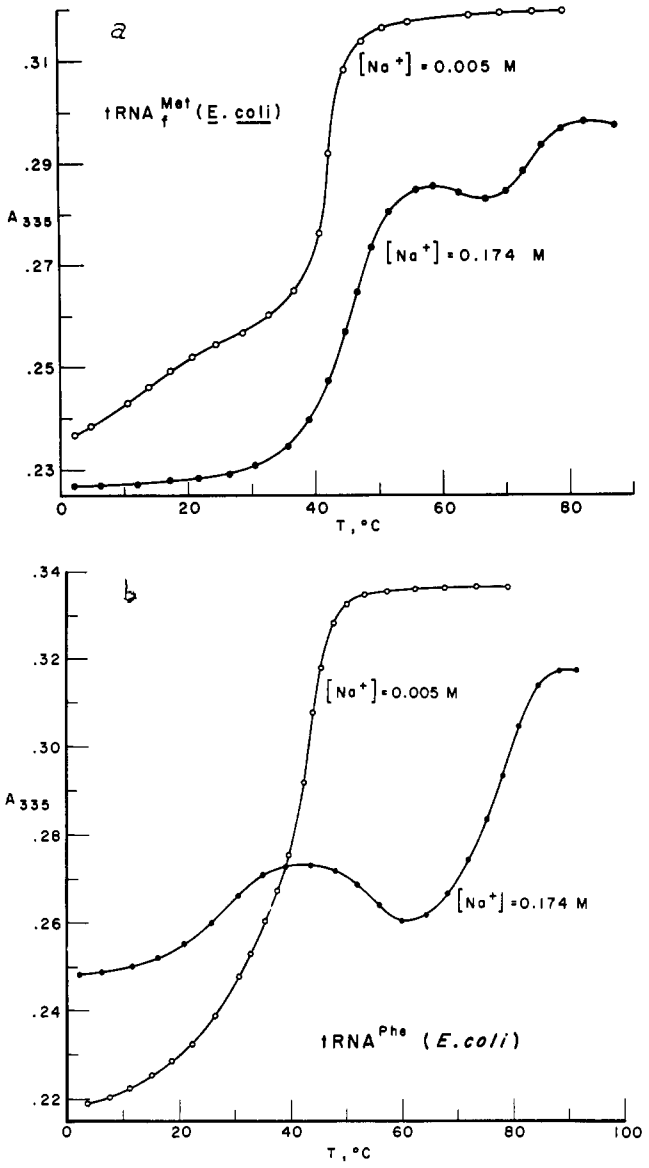

FIGURE 3: Comparison of high- and low-salt melting curves measured at 335 nm. As in Figure 1, absorbance measurements refer to tRNA samples at identical concentrations in high and low salt: (a) $tRNA^{fMet}$, (●) in 0.17 PCEP; (○) in 0.005 PCEP; (b) $tRNA_2^{Phe}$ (●) in 0.17 PCEP; (○) in 0.005 PCEP.

260 nm, for example) or by measuring the absorbance of a minor nucleotide. We report results of both kinds, but we found particularly useful the absorbance at 335 nm, near the absorbance maximum of 4-thiouridine. This minor nucleotide is commonly found at position 8 in *E. coli* tRNA's (at positions 8 and 9 in $tRNA^{Tyr}$ from *E. coli;* Goodman *et al.*, 1968).

The melting curves in Figures 1, 2, and 3 show that at higher Na^+ concentrations (0.17 M, in the presence of EDTA and no added Mg^{2+}) one can reliably detect at least two steps in the melting process. The lower temperature step is seen at 260 nm as a relatively small increase in absorbance (Figures 1a, 2a) but at 335 nm it usually accounts for the largest part of the optical density increase (Figures 1a, 3a). $tRNA^{Phe}$ is the only exception to this latter point (Figure 3b).

At low salt concentrations (0.02 M Na^+ or below, EDTA present) only one step in the melting process can generally be distinguished (Figures 1b, 2b, 3b), although transition

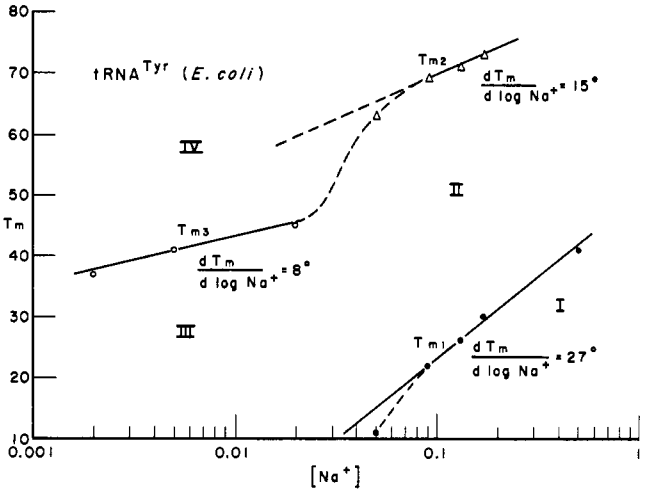

FIGURE 4: Variation of the three transition temperatures (335 nm) for $tRNA_I^{Tyr}$ with the logarithm of sodium ion concentration in PCEP buffer.

curves may be asymmetric and on occasion there is indication of two melting steps (see $tRNA^{fMet}$ at 0.005 M Na^+, measured at 335 nm, Figure 3a).

In order to determine a phase diagram it is necessary to have well-defined melting transitions. It is evident from Figures 1–3 that curves measured at 335 nm are much more useful for this purpose than those measured at 260 nm. In what follows we use T_m values determined at 335 nm; therefore the resulting phase diagram refers, strictly speaking, to the state of the nucleotides that influence the absorbtion spectrum of the 4-thiouridine residue in tRNA. However, this is as good an empirical definition of the state of a tRNA molecule as we have available.

Na^+ Concentration Dependence of T_m Distinguishes Three Different Transitions. We studied in detail the dependence on salt concentration of the melting behavior of $tRNA^{fMet}$ and $tRNA_I^{Tyr}$. Each of these has two well-defined, 335-nm transitions at high Na^+, but only a single resolved transition at low Na^+. Figures 4 and 5 show the variation of the transition midpoints with Na^+ concentration. The three transitions have different slopes on the T_m *vs.* log Na^+ plot, and for $tRNA^{Tyr}$

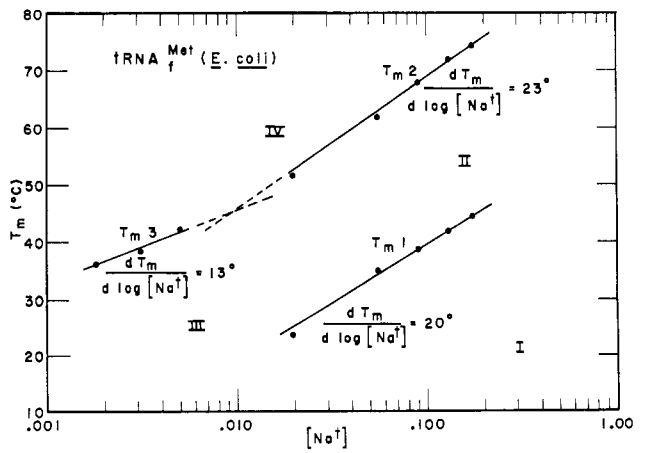

FIGURE 5: Variation of the three transition temperatures (335 nm) for $tRNA^{fMet}$ with the logarithm of sodium ion concentration in PCEP buffer.

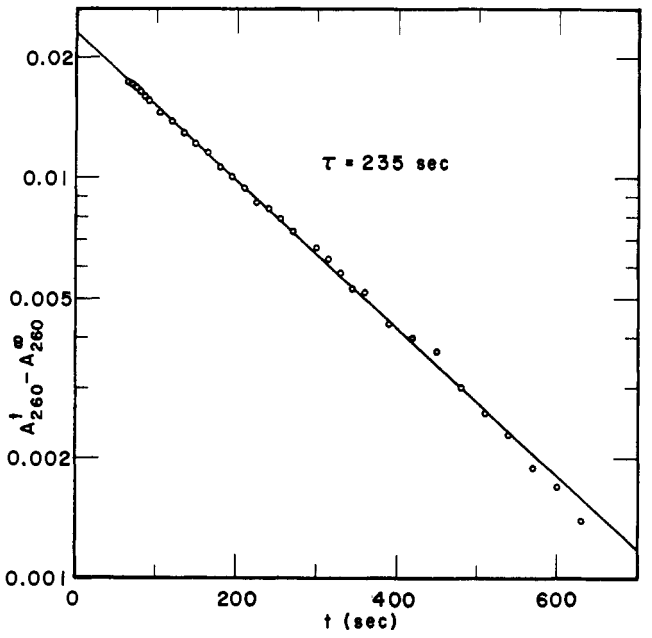

FIGURE 6: Semilogarithmic plot of the absorbance change ($A_{260}^t - A_{260}^\infty$) at 7° as a function of time following a salt jump from Na^+ = 0.012 M to 0.17 M. The tRNA concentration is 1.531 A_{260}/ml measured in 0.012 M Na^+ at 7°. A_{260}^t is the absorbance reading at time t and A_{260}^∞ is the base line when the absorbance reading is constant after the salt jump. The decay decay time τ = 235 sec.

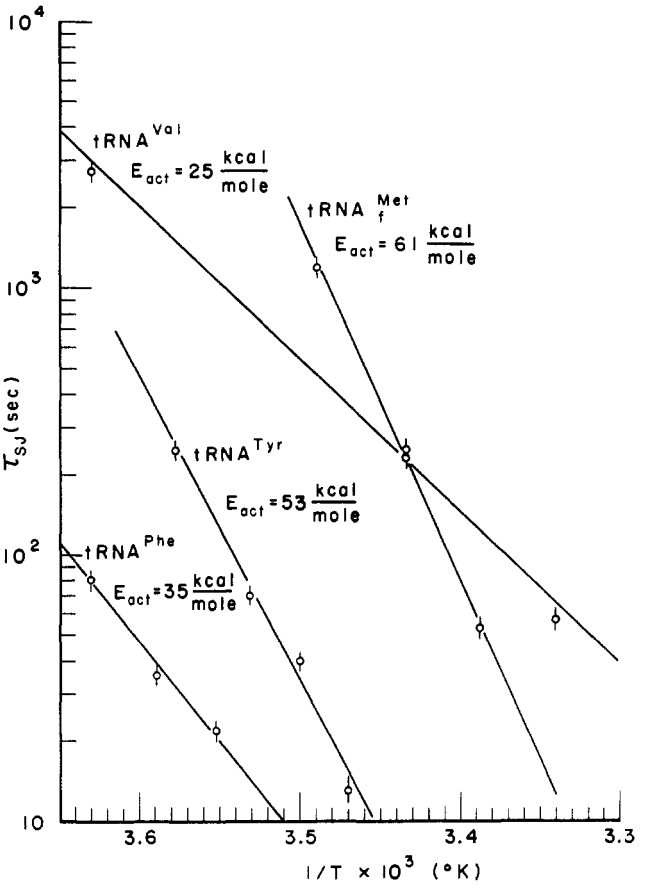

FIGURE 7: Temperature dependence of the salt-jump kinetics for $tRNA^{fMet}$, $tRNA_2^{Phe}$, $tTNA_I^{Val}$ and $tRNA_I^{Tyr}$. For the first three, the conversion was from 0.005 PCEP to 0.17 PCEP; for $tRNA_I^{Tyr}$ the conversion was from 0.02 PCEP to 0.17 PCEP. In the latter case we found no detectable change in time constant τ on changing the initial buffer from 0.02 to 0.012 M Na^+. The figure shows τ plotted on a logarithmic scale against reciprocal temperature.

the lines do not intersect in the region where the slope changes. We conclude that these three processes are different; more specifically, the melting process observed at low salt does not correspond to either of the two processes observed at high salt concentration.

The transition midpoints recorded in Figures 4 and 5 do not agree in every respect with the observations of Seno *et al.* (1969) or Dourlent *et al.* (1971). A possible explanation for this is that our buffers contain EDTA, whereas theirs do not. It is almost impossible to exclude rigorously all contamination by divalent metal ions; the presence of EDTA serves to control the activity of these species. In all cases where there is disagreement, our transition points are lower than theirs. We found our transition temperatures to be reproducible within a few tenths of a degree.

TABLE I: Absorbance Changes and Time Constants for the tRNA Structural Conversion Induced by Salt Jump from 0.005 PCEP to 0.17 PCEP.[a]

tRNA	λ, nm	T, °C	$A_i(\lambda)$	ΔA_{total}	ΔA_{sj}	τ, sec
Phe 2	335	2.2	0.218	0.032	0.024	80
Phe 2	260	2.2	0.635	−0.017	−0.004	
fMet	335	2.2	0.240	−0.010	−0.001	
fMet	260	13.3	0.850	−0.031	−0.012	1184
Val (purified)	260	2.2	0.827	−0.037	−0.020	2500
Val (Oak Ridge)	335	2.2	0.306	−0.032	−0.021	1890

[a] $A_i(\lambda)$ is the initial absorbance at the wavelength λ of measurement; ΔA_{total} is the final absorbance (after addition of salt) minus the initial absorbance; ΔA_{sj} is the amplitude in absorbance units of the slowest kinetic component; τ is the time constant of the slowest exponential component. Absorbance values are corrected for dilution.

These Three Transitions Define a Phase Diagram of Four Zones. The three lines in Figures 4 and 5 break the phase diagram plane into four zones, namely the high-salt, low-temperature form (I), the high-salt, medium-temperature form (II), the low-salt, low-temperature form (III), and the high-temperature form (IV).

When Form III Is Converted to I by "Salt Jump," the Process Has a Large Activation Energy. An important characteristic of the phase diagram is the rate of conversion between various forms, since the kinetic characteristics can be used to diagnose the extent and nature of structural change. We found that when Na^+ (or Na^+ and Mg^{2+}) is added to tRNA in zone III to convert it to zone I, part of the spectral change occurs slowly enough to be measured on the Cary Model 14 spectrophotometer. (Another part of the spectral change is over within a few seconds.) Figure 6 shows a semilogarithmic plot of the absorbance change that results from adding salt to $tRNA_I^{Tyr}$ in zone III. We found that the time constant is independent of tRNA concentration, the tRNA is fully active after the "salt jump," and the melting curve of the resulting tRNA is identical with that measured for a sample dialyzed to form I. The same value of τ, within ±10%, is measured at 260 or 335 nm for $tRNA^{Tyr}$, the only case where the optical

TABLE II: Activation Parameters for Conversion of tRNA from the Low-Salt Form III to Form I (0.17 PCEP), $T = 11°$.[a]

tRNA (*E. coli*)	E_{act} (kcal/mole)	ΔH^+ (kcal/mole)	ΔS^+ (cal/deg per mole)	ΔG^+ (kcal/mole)
fMet	61	60	138	22
Phe 2	35	34	58	18
Val (Oak Ridge)	26	25	18	21
Val (high purity)	25	24	18	21
Tyr	53	52	118	19

[a] The activation energy E_{act} was determined from the decay time τ of the salt jump curve according to $d \log (1/\tau)/dT = E_{act}/(2.303RT^2)$. The other activation parameters were calculated from $1/\tau = (kT/h) \exp (\Delta S^+/R - \Delta H^+/RT)$ where k is the Boltzmann constant and h is Planck's constant. $\Delta G^+ = \Delta H^+ - T\Delta S^+$.

change is sufficiently large to measure at both wavelengths. In contrast, salt concentration changes *within* region III of the phase diagram show no optical effects slow enough to be measured by this technique (dead time, approximately 10 sec).

The slowest exponential component of the optical change following a salt jump is a variable fraction of the total optical change. Depending on tRNA and wavelength, it may be a small or large part of the total; Table I shows some typical values.

When the time constants for conversion from form III to form I are plotted against reciprocal temperature (Figure 7), large activation energies are found. The magnitude of the activation energy depends on the tRNA. In the case of $tRNA^{Phe}$ (35 kcal/mole), $tRNA^{Tyr}$ (52 kcal/mole), and $tRNA^{fMet}$ (61 kcal/mole) the activation energy increases in that order, and the rate decreases correspondingly. $tRNA^{Val}$ (26 kcal/mole) is not a member of this series, since its activation energy is smaller than the others, and its rate is also smaller, except at low temperatures. Table II lists activation parameters for conversion of low-salt forms (III) into form I. It is evident that the conversion of $tRNA^{Val}$ is slow because its entropy of activation is far less favorable than the other tRNA's.

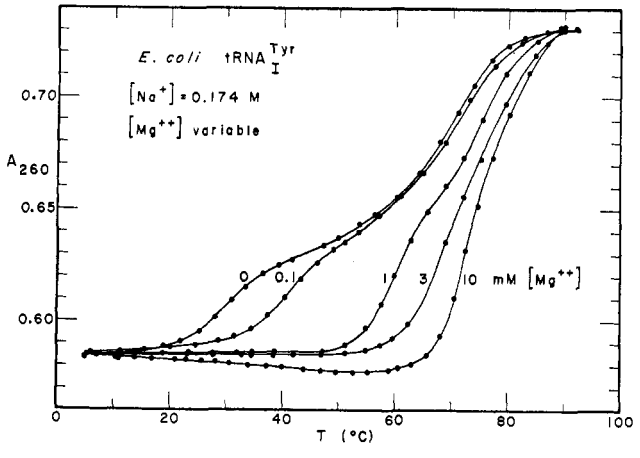

FIGURE 8: Magnesium ion dependence of the melting behavior of $tRNA_I^{Tyr}$ at 260 nm in neutral solutions containing 0.17 M Na^+. PCEP buffers were used, but EDTA was eliminated from the samples containing Mg^{2+}. tRNA samples were dialyzed against the Mg^{2+}-containing buffer. Concentrations of Mg^{2+} are indicated in the figure. All melting curves were arbitrarily normalized by assuming the same absorbance at the lowest temperature.

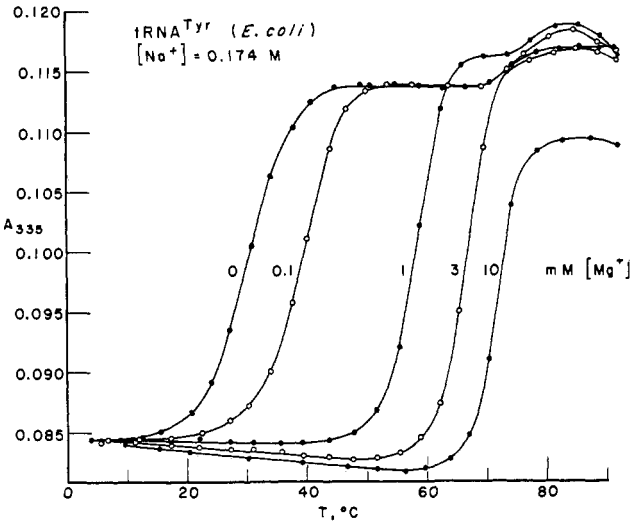

FIGURE 9: Magnesium ion dependence of the melting behavior of $tRNA_I^{Tyr}$ at 335 nm in neutral solutions containing 0.17 M Na^+. Buffers are the same as those described for Figure 8. All melting curves were arbitrarily normalized by assuming the same absorbance at the lowest temperature.

This Activation Energy Implies that Structure Must Be Broken to Convert from Form III to Form I by Salt Jump. The elementary steps of base pair formation have small activation energies (Pörschke and Eigen, 1971; Craig *et al.*, 1971). Hence the probable source of the activation energy in Figure 7 is the heat required to break up the ordered structure that is present in form III (or formed rapidly when salt is added), but not consistent with form I. By analogy with the activation energy for dissociating model double helices (Pörschke and Eigen, 1971; Craig *et al.*, 1971) a larger heat implies that more structure must be broken. A similar activation energy is observed in the related reaction in which "denatured" (inactive)

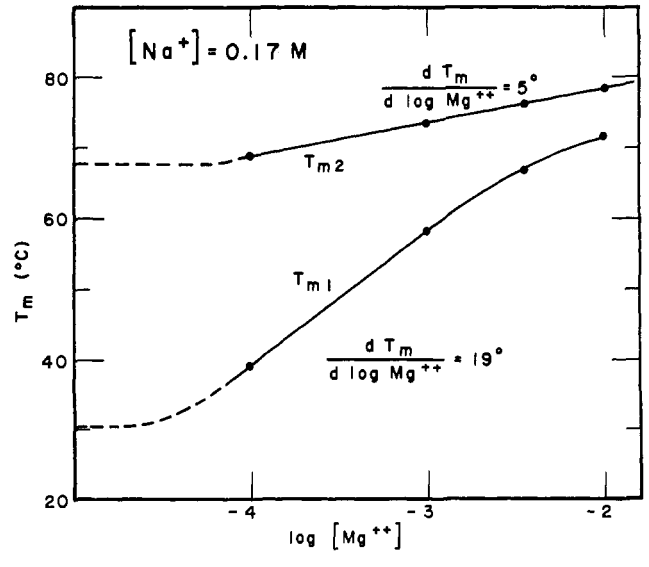

FIGURE 10: Variation of the two high-Na^+ transition temperatures (335 nm) in the presence of varying amounts of Mg^{2+}.

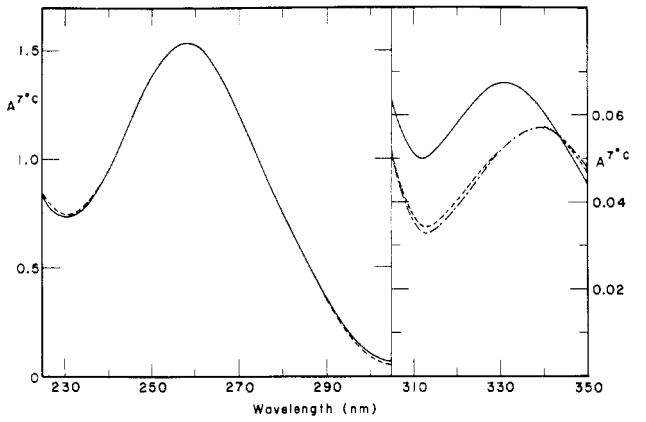

FIGURE 11: Absorbance spectra of $tRNA_I^{Tyr}$ in pH 7 solutions of (——) 0.012 CP, (- - - - -) 0.17 CP, and (-·-·-·-) 0.17 CP + 6 mM $MgCl_2$. CP is a buffer (pH 7) containing 0.1145 M cacodylic acid, 0.01 M NaOH, and the needed amount of $NaClO_4$ to make the desired concentration of Na^+. Spectra were arbitrarily normalized to the same absorbance at 260 nm for all three curves.

tRNA is renatured by heat treatment (Ishida and Sueoka, 1968).

There Is No Evidence for a Separate Mg^{2+} Region of the Phase Diagram. Figures 8 and 9 show transition curves in the presence of variable concentrations of Mg^{2+}, with 0.17 M Na^+. In no case does the character of the high-salt transition change, nor does any new cooperative transition appear. The effect of Mg^{2+} is to increase preferentially the temperature of conversion of form I to II. This effect is summarized in Figure 10, showing a roughly linear variation of each T_m with the logarithm of Mg^{2+} concentration. At high Mg^{2+} the two transitions are compressed together, and a sharp, monophasic transition results.

We also measured the rate of the small optical change that accompanies Mg^{2+} addition to a Na^+-tRNA in form I. We found no detectable effect slower than the dead time of the stopped flow instrument employed. Accordingly, at least 85% (the limit set by the noise level of the instrument) of the small optical change on Mg^{2+} addition occurs within 15 msec.

In contrast, addition of Mg^{2+} and Na^+ together to a low-Na^+ solution of tRNA (form III) yields similar kinetic curves to those seen in converting from form III to I by Na^+ alone; the time constants agree within 30%. It is evident that the conversion from low-Na^+ to high-Na^+ form involves a much more extensive reordering of structural interactions than does addition of Mg^{2+} to the high-Na^+ form.

Conversions among the Forms Show Characteristic Spectral Changes. We studied in detail the influence of salt concentration and temperature on the absorbance spectra of the tRNA samples, and found the following generalizations.

The Position of the Absorbance Maximum near 260 nm Is Virtually Unaffected by Salt Concentration at Constant Temperature, but the Thiouridine Absorbance Maximum Shifts to Higher Wavelengths upon Conversion from III to I. These points are illustrated by Figure 11 for $tRNA_I^{Tyr}$. The wavelengths of maximum absorbance are not appreciably affected by adding Mg^{2+} to form I. Figure 12 shows details of the absorbance change found for addition of Na^+ to form III and Mg^{2+} to form I.

The 4-Thiouridine Absorbance Maximum Shifts to Lower Wavelengths when Temperature Is Increased. As seen in Figure 13, this shift is more pronounced at high Na^+ than low Na^+.

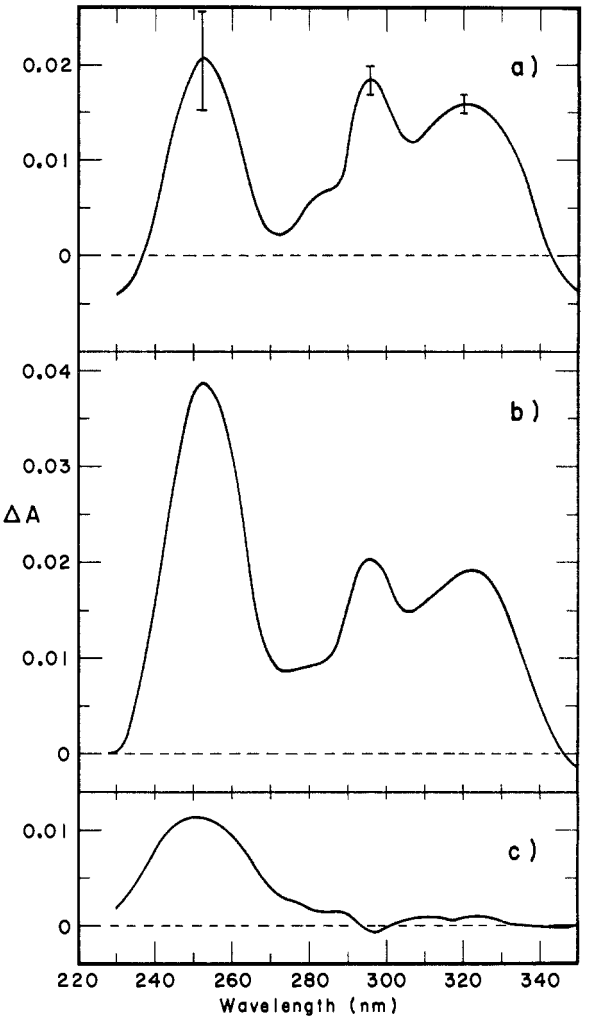

FIGURE 12: Difference spectra upon addition of salt to $tRNA_I^{Tyr}$. A base line was first obtained by measuring the absorbance spectrum with identical tRNA solutions in both sample and reference beams. Concentrated salt was then added to one sample and an equal volume of buffer to the other. A_λ is the absorbance at wavelength λ. $T = 7°$. The buffers are those described in Figure 11. (a) A_λ (tRNA in 0.012 CP) − A_λ (tRNA in 0.17 CP). The concentration of tRNA measured at 7° in 0.012 CP was 1.374 A_{260}/ml. Error bars give the estimated uncertainty. (b) A_λ (tRNA in 0.012 CP) − A_λ (tRNA in 0.17 CP + 5 mM $MgCl_2$). The concentration of tRNA measured at 7° in 0.012 CP was 1.414 A_{260}/ml. (c) A_λ (tRNA in 0.17 CP) − A_λ (tRNA in 0.17 CP + 5 mM $MgCl_2$). The concentration of tRNA measured at 7° in 0.174 CP was 1.446 A_{260}/ml.

Thermal Difference Spectra Show a More "G·C-Rich" Character for Conversion from Form II to IV than for Conversion from Form I to II. This result is illustrated in Figure 14. Further examples are given by Cole (1972). A "G·C-rich" thermal difference spectrum has separate long and short wavelength maxima, whereas the "A·U-rich" spectrum has a single maximum near 260 nm (Fresco *et al.*, 1963; Felsenfeld and Cantoni, 1964).

The Spectral Change for Thermal Melting of Form I to II Is Much Larger than the Change when Mg^{2+} Is Added to Form I. This point, which is important for assessing the effect of Mg^{2+}, is illustrated for $tRNA^{fMet}$ in Figure 15.

Discussion

In order to give a framework for discussion of these results, we present first a working hypothesis of the general

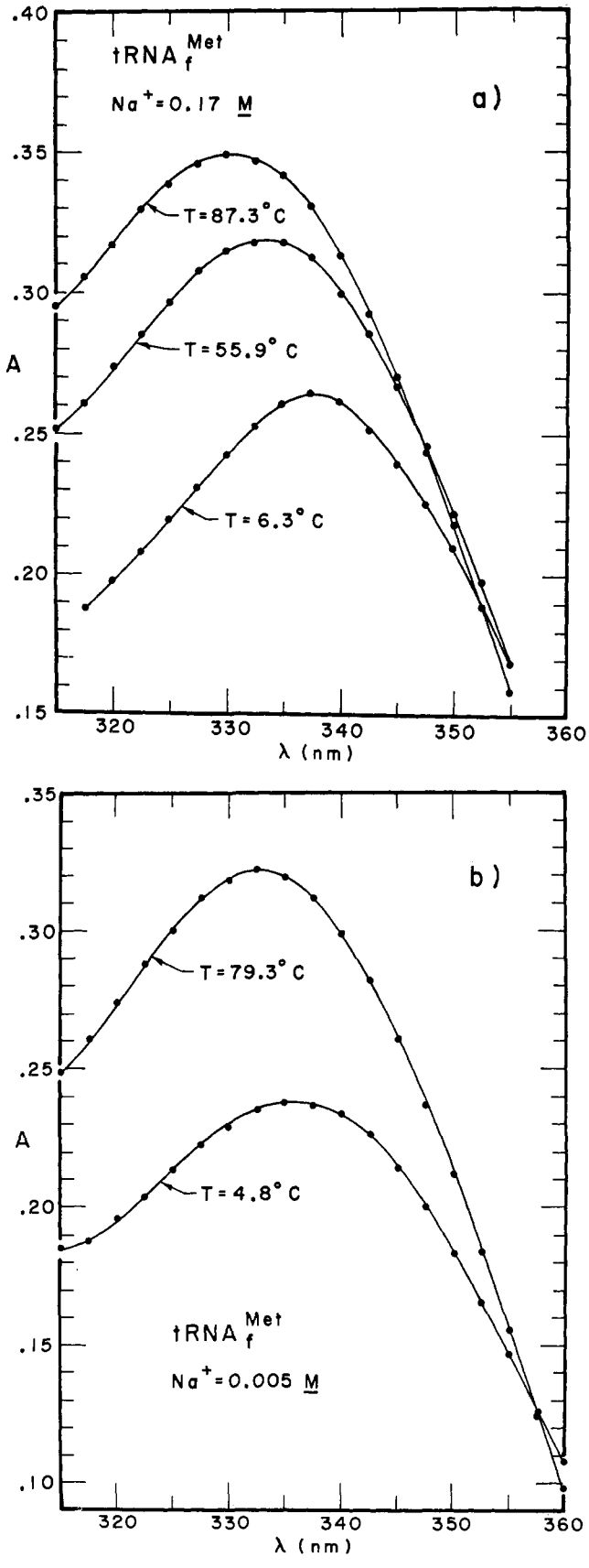

FIGURE 13: Effect of thermal denaturation on the 4-thiouridine absorbance band of $tRNA^{fMet}$: (a) high salt (0.17 PCEP); (b) low salt (0.005 PCEP).

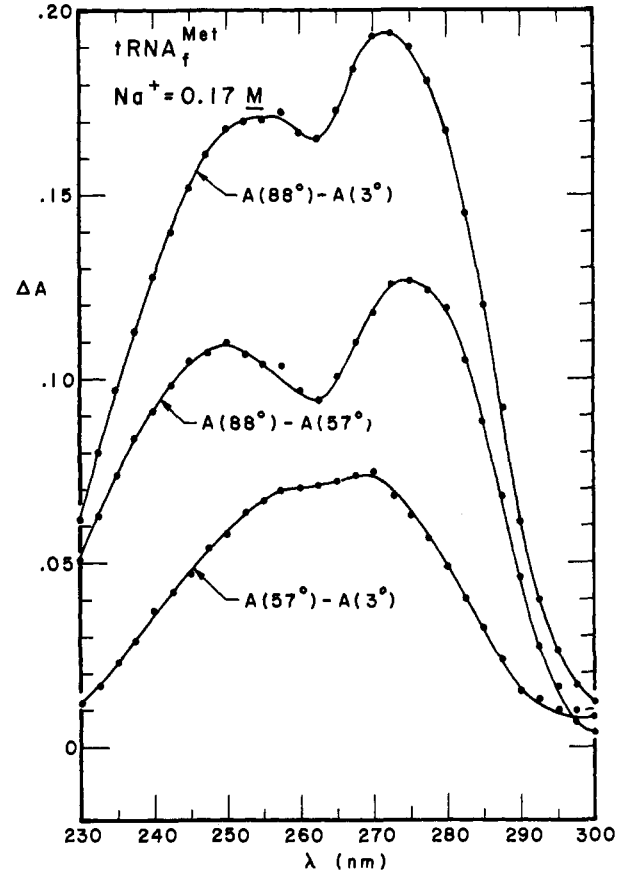

FIGURE 14: Thermal difference spectra for the denaturation of $tRNA^{fMet}$ in 0.17 PCEP. $A(T)$ is the measured absorbance at temperature T. The tRNA concentration measured at 3.0° was 0.77 A_{260}/ml. As seen in Figures 2a and 3a, the intermediate temperature 57° corresponds to completion of the first transition.

nature of the molecular state in each zone of the phase diagram. We emphasize, however, that this diagram should be considered conjectural; presentation of additional evidence that supports it will be continued in later papers.

Figure 16 shows our working hypothesis of the phase diagram for $tRNA^{Tyr}$ and $tRNA^{fMet}$. We equate zone I with "native" tRNA, zone II with cloverleaf or close variants, zone III with "extended forms," and zone IV with the randomly coiling single strand. That zone I is the "native" phase follows from our finding that there is no evidence for a separate Mg^{2+} region of the phase diagram. This does *not* mean that Mg^{2+} produces no structural alterations; the optical changes indicate that it does. However, these optical effects are small and very rapid, and any new structure formed is not a separately melting unit. Mg^{2+} could modify the structure of single-strand regions, add a base pair or two, or modify slightly the geometry of the molecule. However, the cooperatively melting regions present in high Na^+ must remain intact in Mg^{2+}, and no new cooperative region is formed. By this definition, form I is "native."

If form I is the "native" phase, it is natural to expect that the first melting transition will involve loss of the tertiary structure. This is the interpretation first given the low-temperature transition by Fresco *et al.* (1966), largely on the basis of hydrodynamic measurements. However, the reaction has been viewed differently, for example by Römer *et al.* (1970b), who propose that early melting is a cooperative denaturation of tertiary structure and cloverleaf branches, with the acceptor stem melting out *before* the tertiary structure and anticodon helix. (See also Römer *et al.*, 1970.)

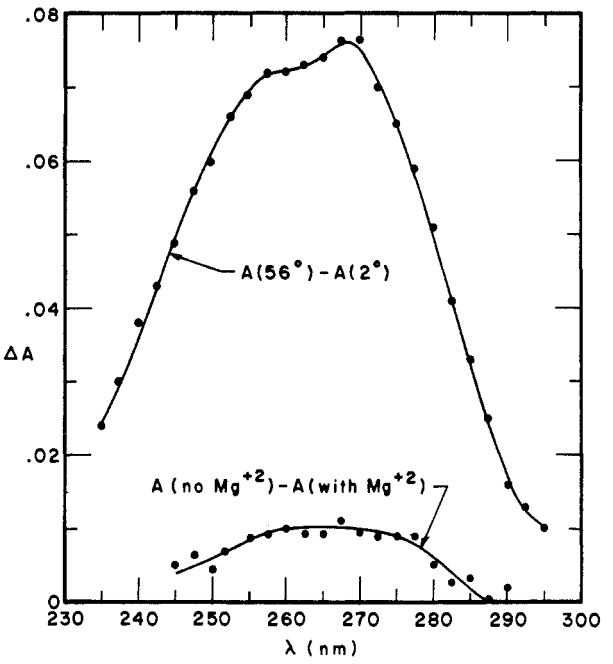

FIGURE 15: Comparison of the absorbance change due to Mg^{2+} addition to $tRNA^{tMet}$ in 0.17 PCEP at 13.2° (lower curve) with the absorbance change due to melting an identical tRNA sample through the first melting transition in 0.17 PCEP. The maximum optical change due to melting is 7–8 times larger than that due to Mg^{2+} addition.

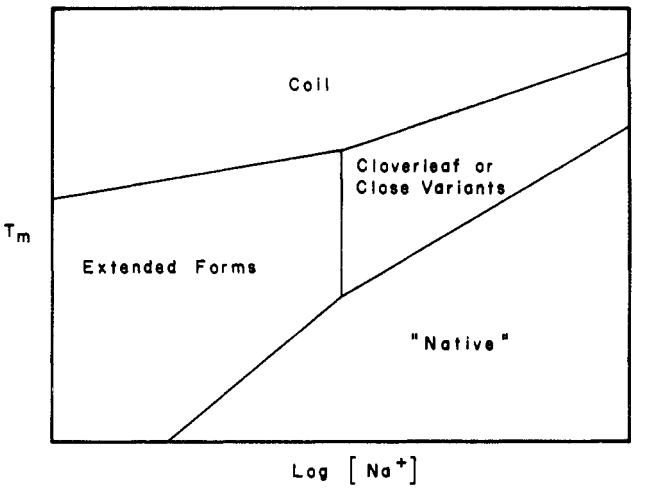

FIGURE 16: Simplified diagram of the hypothesis to explain the phase diagram of tRNA.

The following points of evidence from our work support the original interpretation of Fresco *et al.* (1966). The major absorbance increase at the 4-thiouridine absorbance maximum accompanies the first transition. Since this nucleotide is located in a nonbonded region of the cloverleaf, it is reasonable to suppose that the structure disrupted in the first transition involves noncloverleaf bonding, or tertiary structure.

Thermal difference spectra for the first transition (Figures 14 and 15) imply that the structure broken is less G·C rich than the remainder of the molecule. Since the acceptor stem in $tRNA^{fMet}$ is all G·C pairs, it is unlikely that that helix melts in the first transition. This point is considered more rigorously in the next paper, in which we report thermal difference spectra for all the kinetic components of the first transition.

Application of recently developed stability rules for hairpin helices (DeLisi and Crothers, 1971; Gralla and Crothers, 1972) indicates that the anticodon helix and the TψC helix should be stable to temperatures well above the first transition. We cannot, however, rule out on this basis the possibility that the dihydrouridine helix melts out with the tertiary structure in the first transition.

As detailed in the following paper, the kinetic characteristics of the first transition are not consistent with simple melting of hairpin helices.

As reported in the third paper in the series, tRNA base changes in a nonbonded region of the cloverleaf have a marked effect on the first transition, strongly implying the participation of noncloverleaf (tertiary structure) interactions.

Hence, according to our working hypothesis, the first transition at high salt involves loss of tertiary structure, and we further propose that the product is a cloverleaf or close variant. On this second point our equilibrium studies provide virtually no evidence. In the following paper we show that in some cases there is negligible activation energy involved in converting from II ("cloverleaf") to I ("native"), arguing strongly against the presence of noncloverleaf bonding in II. (The disruption of such "wrong" structure would provide appreciable activation energy for the conversion.) However, it is possible by all our experiments and calculations to date that the least stable part of the cloverleaf, the dihydrouridine helix, could melt out together with the tertiary structure. Such a partly melted cloverleaf is what we would call a "close variant" of the cloverleaf.

In contrast to the rapid kinetics and small activation energy for converting form II ("cloverleaf") to form I ("native") (experiments described in the succeeding paper), the conversion of form III to form I shows slow kinetics and a large activation energy. This strongly implies the existence of bonded structure in form III that is inconsistent with the "native" structure I. This "wrong" bonding might be actually present in III, or rapidly accessible when salt is added.

We call phase III an "extended form" because of the reduced slope of the plot of T_m *vs.* log [Na^+]. This slope is determined by the number of counterions released per calorie of heat in the transition (Crothers, 1971). A small slope for conversion of III to the coil therefore implies a smaller reduction in charge density when III converts to coil than when II converts to coil (assuming the heat of melting is no larger at low than at high salt). Hence the relative charge density on III is less than on II. This may be accomplished by changing the bonding from the compact cloverleaf to some more "extended form"; the conversion occurs in order to reduce the electrostatic free energy when the salt concentration is lowered. A similar suggestion of an extended conformation at low salt was made by Reeves *et al.* (1970).

Hence our general picture of phase III is an extended form with noncloverleaf bonding. Figure 17 shows a specific hypothesis for the nature of the extended forms of $tRNA^{fMet}$, $tRNA_I^{Tyr}$, and $tRNA^{Phe}$. The acceptor and anticodon helix stems remain intact, but the TψC and dihydrouridine helices are broken and a different pairing scheme is imposed. This scheme is supported by our data in two specific ways. The experimental activation energy increases and the observed rate decreases as the extent of "wrong" structure in the model increases, in the order $tRNA^{Phe}$, $tRNA^{Tyr}$, $tRNA^{fMet}$. Since $tRNA^{Val}$ is not a member of this series, we conclude that it

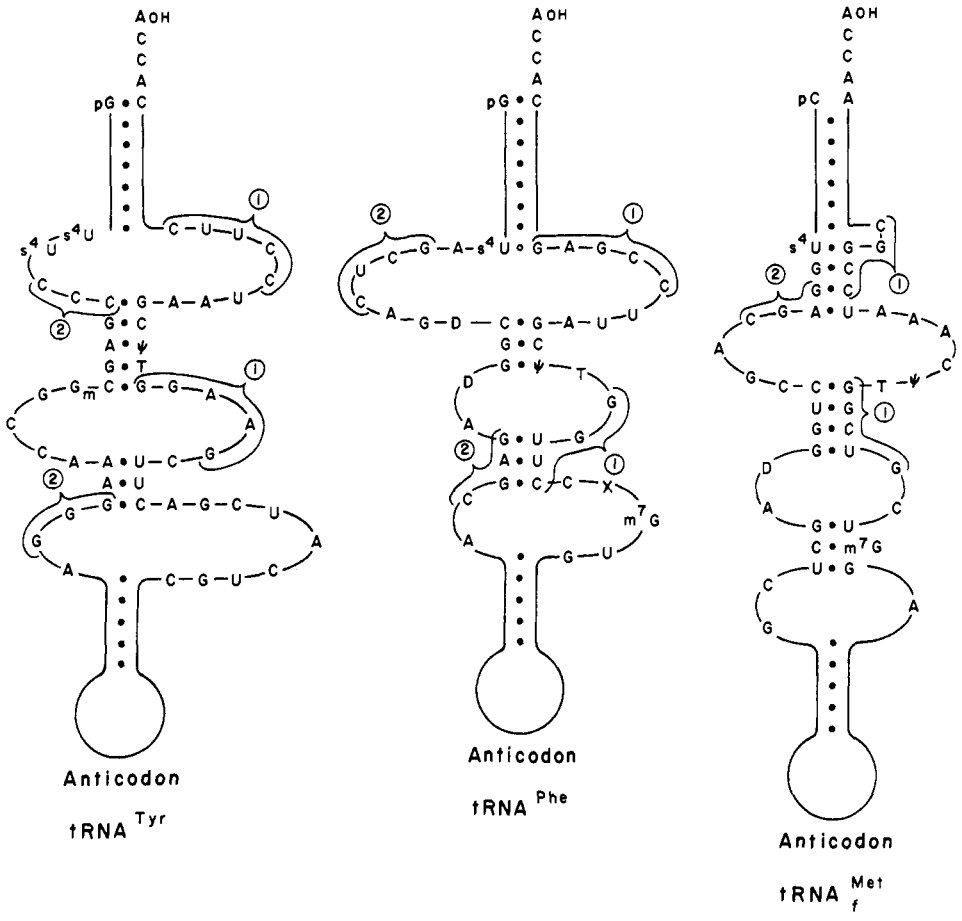

FIGURE 17: Proposed model for the extended forms of $tRNA^{fMet}$, $tRNA_1^{Tyr}$, and $tRNA^{Phe}$. The base pairing in the acceptor stem and anticodon helix is left unaltered, and new pairs are formed in place of the TψC and dihydrouridine helices. Base sequences were determined by Dube *et al.* (1968) and Dube and Marcker (1969) for $tRNA^{fMet}$; by Goodman *et al.* (1968) and RajBhandary *et al.* (1969) for $tRNA^{Tyr}$; and by Barrell and Sanger (1969) for $tRNA^{Phe}$. It should be noted that we are using the sequence of $tRNA^{Phe}$ for a tRNA which Oak Ridge has described as $tRNA_2^{Phe}$. It is not clear whether the $tRNA^{Phe}$ sequence reported by Barrell and Sanger (1969) was obtained from a mixture of isoacceptors or from a purified species.

has a different kind of extended structure. We find that structures of $tRNA^{Val}$ of the type shown in Figure 17 have less pairing than $tRNA^{Phe}$. Hence some other kind of (noncloverleaf) bonded form is preferred at low salt in $tRNA^{Val}$. The model explains the large absorbance increase at 335 nm on melting the "extended form" of $tRNA^{Phe}$, since the 4-thiouridine residue (s^4U) forms a G·s^4U pair at the end of an existing helix. In all other cases the s^4U is not part of a continuous helix in the extended form model.

We consider that form IV is the randomly coiling single strand, with some local stacking interactions intact. The reason for this assignment is analogy with the behavior of polynucleotides, and the fact that no further cooperative melting transitions are observed at higher temperatures.

We conclude with some notes on the expected generality of the phase diagram in Figure 16. We anticipate that most tRNAs will show extended forms at low salt, but the detailed nature of these structures will be strongly sequence dependent. In all cases the electrostatic free energy becomes an important factor at low salt concentration, and leads to preferred structures different from those at high salt.

The "cloverleaf" region of the phase diagram will probably be subject to considerable variation, mainly in the degree of "incorrect" bonding (not consistent with the native form). We anticipate, for example, that denaturable tRNAs such as $tRNA^{Leu}$ (yeast) (Lindahl *et al.*, 1966) and $tRNA^{Trp}$ (*E. coli*) (Gartland and Sueoka, 1966) may not show a cloverleaf region at all. The remarkable variety of conformational possibilities exhibited by tRNA dictates that each species should be examined in detail, without careless assumptions regarding the conformational state.

Acknowledgments

We are grateful to Dieter Söll for continuing advice on the biochemistry of tRNA.

References

Armstrong, D. J., Burrows, W. J., Skoog, F., Roy, K. L., and Söll, D. G. (1969), *Proc. Nat. Acad. Sci. U. S. 63*, 834.

Arnott, S. (1971), *Progr. Biophys. Mol. Biol. 22*, 181.

Barrell, B. G., and Sanger, F. (1969), *FEBS (Fed. Eur. Biochem. Soc.) Lett. 3*, 275.

Cole, P. E. (1972), Thesis, Yale University.

Craig, M. E., Crothers, D. M., and Doty, P. (1971), *J. Mol. Biol. 62*, 383.

Cramer, F. (1971), *Progr. Nucl. Acid Res. Mol. Biol. 11*, 391.

Crothers, D. M. (1971), *Biopolymers 10*, 2147.

DeLisi, C., and Crothers, D. M. (1971), *Biopolymers 10*, 1809.

Dourlent, M., Yaniv, M., and Helene, C. (1971), *Eur. J. Biochem. 19*, 108.

Dube, S. K., and Marcker, K. A. (1969), *Eur. J. Biochem. 8*, 256.
Dube, S. K., Marcker, K. A., Clark, B. F. C., and Cory, S. (1968), *Nature (London) 218*, 232.
Eisinger, J., Feuer, B., and Yamane, T. (1971), *Nature (London), New Biol. 231*, 126.
Felsenfeld, G., and Cantoni, G. L. (1964), *Proc. Nat. Acad. Sci. U. S. 51*, 818.
Felsenfeld, G., and Sandeen, G. (1962), *J. Mol. Biol. 5*, 587.
Fresco, J. R., Adams, A., Ascione, R., Henley, D., and Lindahl, T. (1966), *Cold Spring Harbor Symp. Quant. Biol. 31*, 527.
Fresco, J. R., Klotz, L. C., and Richards, E. G. (1963), *Cold Spring Harbor Symp. Quant. Biol. 28*, 83.
Gartland, W. J., and Sueoka, N. (1966), *Proc. Nat. Acad. Sci. U. S. 55*, 948.
Goodman, H. M., Abelson, J., Landy, A., Brenner, S., and Smith, J. D. (1968), *Nature (London) 217*, 1019.
Gralla, J., and Crothers, D. M. (1972), *J. Mol. Biol.* (in press).
Hoskinson, R. M., and Khorana, H. G. (1965), *J. Biol. Chem. 240*, 2129.
Ishida, T., and Sueoka, N. (1968), *J. Biol. Chem. 243*, 5329.
Lindahl, T., Adams, A., and Fresco, J. R. (1966), *Proc. Nat. Acad. Sci. U. S. 55*, 941.
Nishimura, S., Harada, F., Narushima, U., and Seno, T. (1967), *Biochim. Biophys. Acta 142*, 133.
Pörschke, D., and Eigen, M. (1971), *J. Mol. Biol. 62*, 361.
RajBhandary, U. L., Chang, S. H., Gross, H. J., Harada, F., Kimura, F., and Nishimura, S. (1969), *Fed. Proc., Fed. Amer. Soc. Exp. Biol. 28*, 409.
Reeves, R. H., Cantor, C. R., and Chambers, R. W. (1970), *Biochemistry 9*, 3993.
Riesner, D., Römer, R., and Maass, G. (1969), *Biochem. Biophys. Res. Commun. 35*, 369.
Römer, R., Riesner, D., Coutts, S. M., and Maass, G. (1970a), *Eur. J. Biochem. 15*, 77.
Römer, R., Riesner, D., and Maass, G. (1970b), *FEBS (Fed. Eur. Biochem. Soc.) Lett. 10*, 352.
Seno, T., Kobayashi, M., and Nishimura, S. (1969), *Biochim. Biophys. Acta 174*, 71.
Strittmatter, P. (1964), *in* Rapid Mixing and Sampling Techniques in Biochemistry, Chance, B., Eisenhardt, R., Gibson, Q., and Lonberg-Holm, K., Ed., New York, N. Y., Academic Press, p 76.
Uhlenbeck, O. C., Baller, J., and Doty, P. (1970), *Nature (London) 225*, 508.
Yang, S. K. (1972), Thesis, Yale University.
Yang, S. K., Söll, D. G., and Crothers, D. M. (1972), *Biochemistry 11*, 2311.

Conformational Changes of Transfer Ribonucleic Acid. Relaxation Kinetics of the Early Melting Transition of Methionine Transfer Ribonucleic Acid (*Escherichia coli*)†

P. E. Cole and D. M. Crothers*

ABSTRACT: We report temperature-jump studies of the early melting transition of $tRNA^{fMet}$ (*Escherichia coli*). There are two measurable relaxation times τ, both independent of concentration and visible at 266 and 335 nm. The temperature dependence of the τ values establishes apparent activation energies, and implies that the process of structure formation has negligible activation energy, while dissociation of structure requires energy. We also measured the thermal difference spectrum for both relaxation effects, and found that each of these is apparently less G·C rich than the total tRNA melting. These results allow a general comparison of the rate of regenerating the "native" structure (zone I of the tRNA phase diagram), either from the low-salt (zone III) form, or from the zone II form (the product of the early melting transition). The conversion from the low-salt form is several orders of magnitude slower, and has a much larger activation energy. We conclude that zone II and zone III represent different conformations. Further consideration of all the factors leads to the conclusion that zone II is a structure with no noncloverleaf bonding, but in which the dihydrouridine helix of the cloverleaf may be melted. The kinetic results imply that the tertiary structure of $tRNA^{fMet}$ contains at least two regions of interaction whose melting is not obligatorily coupled. We present a simple hypothesis to interpret the results further, in which there are two interaction regions whose melting is virtually independent. With this hypothesis, we find that (in 0.17 M Na^+) region 1 is formed in approximately 2–3 msec, and has a dissociation heat of about 22 kcal/mole, while region 2 is formed in about 7 msec, and has a dissociation heat of 51 kcal/mole. The melting of region 2 may include opening of the dihydrouridine helix, but all other interactions involve tertiary structure.

The most interesting current questions about tRNA structure involve the nature of the tertiary folding (Arnott, 1971). In the previous paper (Cole *et al.*, 1972) we used equilibrium and kinetic measurements to develope a conformational phase diagram, in which it was proposed that the low-temperature melting process seen at high Na^+ concentration

† From the Department of Chemistry, Yale University, New Haven, Connecticut. *Received June 9, 1972.* This is the second paper in a series; the preceding paper was by Cole *et al.* (1972). This work was supported by a grant (GM 12589) from the National Institutes of Health. D. M. C. holds a Career Development award (GM 19978) from the same source. P. E. C. was supported by NIH Predoctoral Fellowship GM 41629.